INTERNATIONAL JOURNAL FOR NUMERICAL METHODS IN FLUIDS
Int. J. Numer. Meth. Fluids 2008; **56**:1449–1456
Published online 13 September 2007 in Wiley InterScience (www.interscience.wiley.com). DOI: 10.1002/fld.1614

Fluid flow simulation at open–porous medium interface using the lattice Boltzmann method

A. Nabovati*, † and A. C. M. Sousa

Department of Mechanical Engineering, University of New Brunswick, Fredericton, NB, Canada E3B 5A3

SUMMARY

The present study investigates, using the lattice Boltzmann method, the influence on the flow of the boundary condition at the open and porous medium interface for a two-dimensional channel with half of the channel filled with a random porous medium. By simulating the fluid flow at pore level, the proposed macroscopic hydrodynamic boundary conditions are evaluated; correlations for the empirical constant in one of the most widely used models are also presented. The predicted values for the flow rate are in overall agreement with the previously published values. Copyright © 2007 John Wiley & Sons, Ltd.

Received 22 March 2007; Revised 2 August 2007; Accepted 3 August 2007

KEY WORDS: open porous interface; pore level analysis; lattice Boltzmann method

1. INTRODUCTION

The present study investigates the boundary condition at the open and porous medium interface for a two-dimensional channel with half of the channel filled with a random porous medium. The fluid flow was simulated using the lattice Boltzmann method (LBM); periodic boundary conditions were applied at the inlet and outlet of the channel, indicating that the flow is fully developed in both open and porous medium and the net spanwise flow at the interface is zero. This requires the region under study to be far from the inlet and outlet boundaries and the pressure gradient to be equal in the streamwise direction in both porous and open regions. One of the main applications of the interfacial flow simulation is in the resin transfer molding (RTM) process [1, 2], where

*Correspondence to: A. Nabovati, Department of Mechanical Engineering, University of New Brunswick, Fredericton, NB, Canada E3B 5A3.
†E-mail: a.nabovati@unb.ca

Contract/grant sponsor: Foundation for Science and Technology (FCT, Portugal); contract/grant number: POCTI/EME/59728/2004
Contract/grant sponsor: NSERC (Natural Sciences and Engineering Research Council of Canada); contract/grant number: 12875

the flow at the open gap existing between the porous preform matrix and the mold creates a preferential flow passage for the resin, which may cause the incomplete wetting of the fibers and void formation and reduces the quality of the produced parts dramatically. The first systematic analysis of the fluid flow at the interface of the open and porous region was done by Beavers and Joseph [3]; since then interfacial fluid flow and heat transfer have received considerable attention. In the model presented by Beavers and Joseph [3] the interfacial shear stress was related to the slip velocity at the interface and the average velocity in the porous medium is given as follows:

$$\left.\frac{\mathrm{d}u}{\mathrm{d}y}\right|_{+} = \frac{\alpha}{\sqrt{K}}(u_{\mathrm{int}} - \langle u\rangle_{\mathrm{porous}}) \tag{1}$$

where α is an empirical constant, namely slip coefficient, K the porous medium permeability, u_{int} velocity at the interface and $\langle u\rangle_{\mathrm{porous}}$ the volume averaged velocity in the porous medium; $\mathrm{d}u/\mathrm{d}y|_{+}$ denotes the velocity profile slope at the interface approaching from the open side. Equation (1) indicates that the shear stress is continuous at the interface, if the interface boundary layer thickness is assumed to be of the order of $\sqrt{K}$ [4] at the porous side.

Vafai and Thiyagaraja [5] analytically solved the fluid flow and heat transfer at three different interface configurations, namely interface of two different porous media, interface of a porous medium and an open region and interface of an impermeable wall and a porous medium. In their work, continuity of the velocity field and the shear stress at the interface was employed to calculate the slip velocity at the interface. Reported results were in agreement with the model of Beavers and Joseph [3]. Sahraoui and Kaviany [6] studied the boundary condition for the interfacial flow at pore level assuming that the porous medium was made of two-dimensional regularly ordered cylinders. Numerically solving the flow field near the interface, it was shown that the slip coefficient introduced by Beavers and Joseph [3] is an increasing function of the porosity and its magnitude is around 1. Alazmi and Vafai [7] presented a review of different hydrodynamic and thermally interfacial boundary conditions and discussed the merits and drawbacks of each. Costa *et al.* [8] applied a finite volume finite element method to study the two-dimensional fluid flow in the adjacent open and porous domains; they solved the Brinkman–Forchheimer equation in the porous medium and the Navier–Stokes equations in the open domain.

In the present study, no assumption was made for the fluid flow at the interface and in the porous region; therefore, the simulation results can be used to verify the available models and find the dependence of the slip coefficient to the problem parameters.

2. METHODOLOGY

Fluid flow in the two-dimensional random porous media was simulated at pore level using the single relaxation time LBE [9, 10]; the evolution equation of the particles, which governs the fluid dynamics, expressed in the following form:

$$f_i(\mathbf{x}+c_i\delta t, t+\delta t) = -\omega[f_i(\mathbf{x},t) - f_i^{\mathrm{eq}}(\mathbf{x},t)] \tag{2}$$

where δt, ω and c_i are the lattice time step, inverse of the lattice relaxation time and the lattice discrete velocity set. The particle distribution function, f, has directional components on each lattice site and it represents the probability of finding a fluid particle at position $\mathbf{x}$, time t and

DOI: 10.1002/fld

direction of c_i [11]. The macroscopic density and velocity on each lattice site are calculated using the distribution function on that site and the neighboring sites as follows:

$$\rho = \sum f_i = \sum f_i^{\mathrm{eq}} \tag{3}$$

$$\rho \mathbf{u} = \sum c_i f_i = \sum c_i f_i^{\mathrm{eq}} \tag{4}$$

The most common two-dimensional lattice is the D2Q9 lattice, which was also used in this study, where '2' denotes the number of space dimensions and '9' refers to the discrete set of nine velocities as proposed by Qian *et al.* [9]. For the D2Q9 lattice, the discrete velocity set is formulated as follows:

$$C_i = \begin{cases} 0, & i = 0 \\ c[\cos((i-1)\pi/2), \sin((i-1)\pi/2)], & i = 1,2,3,4 \\ \sqrt{2}c[\cos((2i-1)\pi/4), \sin((2i-1)\pi/4)], & i = 5,6,7,8 \end{cases} \tag{5}$$

where $c = \delta x/\delta t$ and δx is the lattice length scale; in most of the LBM simulations on uniform lattices, δx and δt are considered, for simplicity, to be equal to one. The selected equilibrium distribution function should satisfy the conservation of mass and momentum, and it should ensure that fluid isotropy and Galilean invariance are achieved. For the D2Q9 lattice, the discrete equilibrium distribution function is in the form of a second-order truncated expansion of Maxwell–Boltzmann equilibrium function, namely

$$f_i^{\mathrm{eq}} = \rho \lambda_i \left[1 + \frac{3}{c^2} c_i.\mathbf{u} + \frac{9}{2c^4} (c_i.\mathbf{u})^2 - \frac{3}{2c^2} \mathbf{u}.\mathbf{u} \right] \tag{6}$$

where λ_i is the weighting factor, which is defined as

$$\lambda_i = \begin{cases} 4/9 & \text{if } i = 0 \\ 1/9, & i = 1,2,3,4 \\ 1/36, & i = 5,6,7,8 \end{cases} \tag{7}$$

The temporal evolution of the distribution function at each time step is realized through a two-step approach consisting of streaming and collision. The corresponding fluid viscosity is calculated using the inverse of the relaxation time and the lattice sound speed, namely

$$v = \left(\frac{1}{\omega} - \frac{1}{2} \right) c_{\mathrm{s}}^2 \tag{8}$$

In a D2Q9 lattice the speed of sound is $c_{\mathrm{s}} = c/\sqrt{3}$, and the pressure on each lattice site can be evaluated using the equation of state of an ideal gas as follows:

$$p = \rho c_{\mathrm{s}}^2 \tag{9}$$

The periodic boundary condition was applied in the x-direction. Solid-wall boundary conditions are set at the top and bottom wall with the bounce back method. The solid obstacles were also implemented using the bounce back method at their surface; consequently, the actual solid wall falls in the midway of the link between the solid and fluid nodes. The porosity was defined as the ratio of the fluid nodes to the total number of the nodes (excluding side walls); therefore, the position of the solid boundaries does not affect the porosity.

DOI: 10.1002/fld

3. RESULTS

The very first challenge in pore level analysis is to determine the structure of the medium at pore level. Applied experimental and imaging techniques have had some success in the determination of these structures [12]; even so, experimental methods have their own limitations and, in general, are costly. An alternative approach, which has been popular with many researchers in this field, is to simulate the fluid flow in a reconstructed virtual medium capable of reproducing the real medium behavior. The medium can be formulated, as a first approximation, by considering ordered or random packing of two- or three-dimensional objects. Figure 1(a) shows the random porous medium structure and the boundary conditions used in this study; the two-dimensional square obstacles with a uniform random distribution were placed with free overlapping in the porous medium region. The two-dimensional geometry assumption may impose limitations on the applicability of the predicted parameters; however, it should be noted that the majority of analytical studies and also a considerable number of numerical and experimental work have been restricted to two-dimensional cases. To establish a sharp interface edge, the obstacles at the interface are truncated. Having created a truncated sharp interface, ambiguity in the location of the true interface associated with past works, where the porous medium is assumed to be a structure with ordered obstacles and effect of the interface location on the calculated boundary condition [6], is removed. Figure 1(b) shows the dimensionless average velocity profile in the open and porous region for three different porosities and for the case that there is an impermeable wall at the interface (a medium of zero porosity); the velocity was made dimensionless by using the maximum velocity in the open channel for an

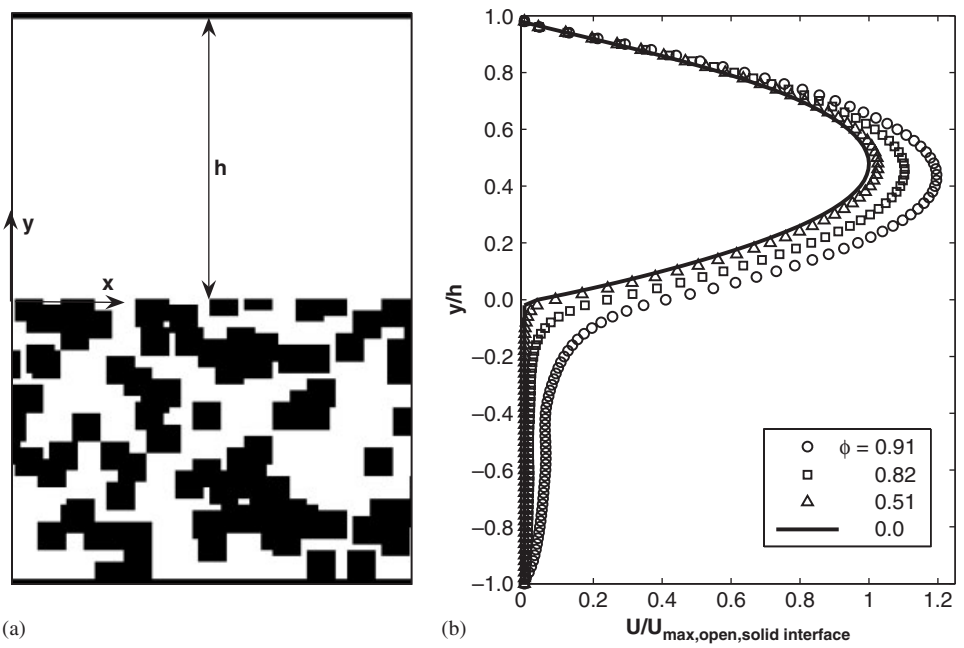

Figure 1. (a) Model structure and (b) non-dimensional velocity profile in the open and porous region for three different porosities and an impermeable wall.

DOI: 10.1002/fld

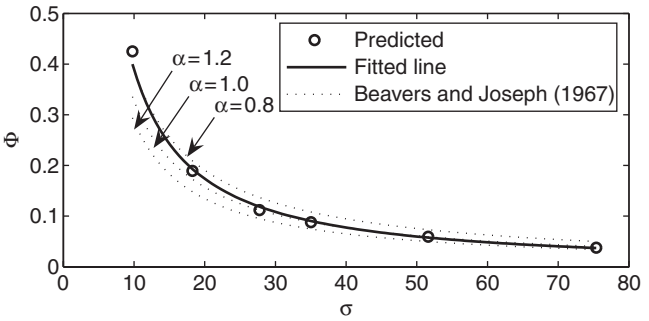

Figure 2. Calculated dimensionless flow rate and comparison with the correlation of Beavers and Joseph [3] for three different values of the slip coefficient.

impermeable wall interface case. As shown in this figure, the velocity and its derivative in spanwise direction, hence the shear stress, are continuous at the interface for the porosities investigated in this study; by increasing the porosity, the slip velocity at the interface and the average velocity in the open and porous region also increase. The permeability of the porous medium was estimated using the Darcy law while the average velocity in the porous medium was calculated by averaging the superficial velocity throughout the porous medium, including the decelerating effect of the wall and accelerating effect of the slip velocity at the interface. The average velocity profile in the porous region clearly shows that the effect of the interface is more pronounced than the effect of the solid wall, thus causing the average velocity in the porous medium to be higher than the Darcy velocity. The agreement between Vafai and Thiyagaraja [5] analysis and the present computations of the slip velocity at the interface are within 5% for values of σ larger than 9, when the assumption of a Poiseuille flow in the open channel is nearly satisfied.

Increase in the open region flow rate due to the presence of the permeable boundary condition was reported in the form of a dimensionless parameter Φ by Beavers and Joseph [3] as follows:

$$\Phi = \frac{\dot{Q} - \dot{Q}_s}{\dot{Q}_s} \tag{10}$$

where $\dot{Q}$ and $\dot{Q}_s$ are the flow rate in the open area where there are permeable and impermeable walls. Using the slip coefficient defined in Equation (1), Beavers and Joseph [3] reported the following correlation for Φ:

$$\Phi = \frac{3(\sigma + 2\alpha)}{\sigma(1 + \alpha\sigma)} \tag{11}$$

where σ is $h/\sqrt{K}$ and h is the channel height; the slip coefficient, α, depends on the porous medium structure and different values of order of 1 was reported for different porous medium structures. The predicted values for the parameter Φ are shown in Figure 2 and they are compared with the values obtained using Equation (11) and three different values of the slip coefficient.

DOI: 10.1002/fld

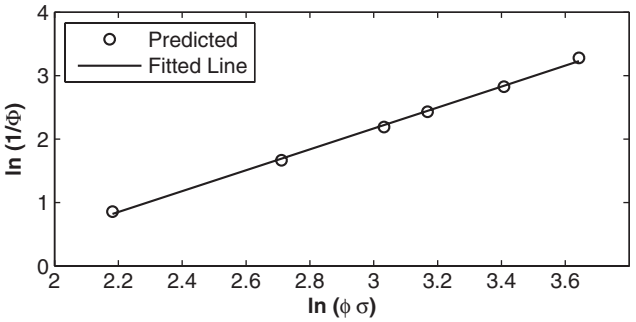

Figure 3. Log–log graph of $1/\Phi$ *versus* $\phi\sigma$.

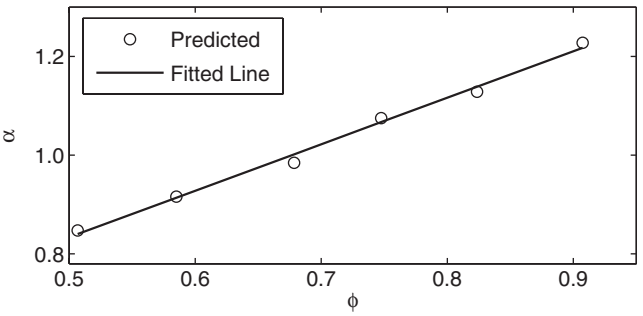

Figure 4. Predicted slip coefficient as a function of the porosity and the polynomial fit.

The form of the Φ–σ plot suggests a logarithmic relation of Φ to σ; to formulate this relation $1/\Phi$ was used as the argument of the logarithm function; Figure 3 reports on the log–log graph of $1/\Phi$ *versus* $\phi\sigma$. The dimensionless flow rate can be best predicted using the following relation:

$$\ln(1/\Phi) = 1.6488 \ln(\phi\sigma) - 2.7791 \tag{12}$$

Sahraoui and Kaviany [6] found that the slip coefficient is a function of different parameters, namely porosity, particle Reynolds number, interface position selection and interfacial particle arrangement. In the present study, a random structure for the porous media was used, which is a reasonable approximation of the complex structure of the actual porous media at the pore level. By leveling the interface, the slip coefficient does not depend either on the interface position selection or the particle arrangement. The particle Reynolds number in the present study was of order of 10^{-3}, which is below the reported value for the lower threshold, 10^{-1} as reported by Sahraoui and Kaviany [6], of the Reynolds number effectiveness region. To determine the slip coefficient in Equation (1), the interface velocity was directly obtained from the simulation results. The derivative of the velocity at the interface is calculated assuming that the boundary condition is only spatially dependent, and a polynomial of order $2n$ is fitted to the predicted data; the nodes employed include n nodes above the interface and n nodes below the interface and the interface node. Results showed negligible sensitivity to the number of the nodes accounted for the polynomial fitting; a polynomial of order 10 was used to calculate the velocity derivative at the interface. Using the data obtained

DOI: 10.1002/fld

from the simulations, the slip coefficient was calculated for different porosities and the result is depicted in Figure 4; it can be seen that the predicted slip coefficient is of a magnitude close to 1 and is an increasing function of the porosity.

The simulation results for the slip coefficient can be correlated as a linear function of the porosity as follows:

$$\alpha = 0.942\phi + 0.3625 \tag{13}$$

4. CONCLUSION

In the present work, fluid flow was simulated in a channel partially filled by a porous medium using the LBM with the objective of investigating the flow characteristics at interface of the open and porous medium at the pore level. No assumption was made for the flow condition at the interface; therefore, the results of the simulation can be used to validate the conditions at the interface that have been in the literature for some time. Using the simulation results, it was found that the slip coefficient is a function of the porosity; the simulation data set was correlated for the slip coefficient as a function of the medium porosity. As expected, the implementation of a permeable wall boundary condition increased the overall flow rate in comparison with the impermeable wall case. The dimensionless flow rate was in good general agreement with the correlation suggested on an experimental basis by Beavers and Joseph [3]; it was found that the logarithm of the non-dimensional flow rate increased linearly as a function of the logarithm of $\phi\sigma$; a correlation is proposed for this relation.

ACKNOWLEDGEMENTS

The authors acknowledge the support received from the Foundation for Science and Technology (FCT, Portugal) through the research grant POCTI/EME/59728/2004 (ACMS) and from NSERC (Natural Sciences and Engineering Research Council of Canada) Discovery Grant 12875 (ACMS).

REFERENCES

1. Aghakhanlou A. Flow development at open and porous region interfaces. *M.Sc. Dissertation*, Department of Mechanical Engineering, University of New Brunswick, 2006.
2. Song YS. Mathematical analysis of resin flow through fibrous porous media. *Applied Composite Materials* 2006; **13**(5):335–343.
3. Beavers GS, Joseph DD. Boundary conditions at a naturally permeable wall. *Journal of Fluid Mechanics* 1967; **30**:197–207.
4. Kaviany M. *Principles of Heat Transfer in Porous Media*. Springer: New York, 1991.
5. Vafai K, Thiyagaraja R. Analysis of flow and heat transfer at the interface region of a porous medium. *International Journal of Heat and Mass Transfer* 1987; **30**(7):1391–1405.
6. Sahraoui M, Kaviany M. Slip and no slip velocity boundary conditions at interface of porous, plain media. *International Journal of Heat and Mass Transfer* 1992; **35**(4):927–943.
7. Alazmi B, Vafai K. Analysis of fluid flow and heat transfer interfacial conditions between a porous medium and a fluid layer. *International Journal of Heat and Mass Transfer* 2001; **44**:1735–1749.
8. Costa VAF, Oliveira LA, Baliga BR, Sousa ACM. Simulation of coupled flows in adjacent porous and open domains using a control-volume finite-element method. *Numerical Heat Transfer—Part A* 2004; **45**:675–697.

DOI: 10.1002/fld

9. Qian YH, d'Humieres D, Lallemand P. Lattice BGK model for Navier–Stokes equation. *Europhysics Letters* 1992; **17**(6):479–484.
10. Succi S. *The Lattice Boltzmann Equation—For Fluid Dynamics and Beyond*. Oxford University Press: Oxford, 2001.
11. Succi S, Filippova O, Chen H, Orszag S. Towards a renormalized lattice Boltzmann equation for fluid turbulence. *Journal of Statistical Physics* 2002; **107**(1/2):261–278.
12. Hejis AWJ, Lowe CP. Numerical evaluation of the permeability and the Kozeny constant for two types of porous media. *Physical Review E* 1995; **51**:4346–4353.

DOI: 10.1002/fld